# Hydrogen impurities and shallow donors in SnO_{2} studied by infrared spectroscopy

Figen Bekisli, Michael Stavola, W. Beall Fowler, Lynn Boatner, Erik Spahr, and Gunter Lüpke

**Hydrogen impurities and shallow donors in SnO$_2$ studied by infrared spectroscopy**

Figen Bekisli,[1] Michael Stavola,[1,*] W. Beall Fowler,[1] Lynn Boatner,[2] Erik Spahr[3] and Gunter Lüpke[3]

[1]Department of Physics and the Sherman Fairchild Laboratory, Lehigh University, Bethlehem, Pennsylvania 18015, USA

[2]Oak Ridge National Laboratory, Materials Science and Technology Division, Oak Ridge, Tennessee 37831, USA

[3]Department of Applied Science, College of William and Mary, Williamsburg, Virginia 23187, USA

Abstract

Hydrogen has been found to be an important source of n-type conductivity in the transparent conducting oxide SnO$_2$. We have studied the properties of H in SnO$_2$ single crystals with infrared spectroscopy. When H or D is introduced into SnO$_2$ by annealing in an H$_2$ or D$_2$ ambient at elevated temperature, several O-H and O-D vibrational lines are produced along with the low-frequency absorption that is characteristic of free carriers. To probe the relationship between H and the free carriers it introduces, the thermal stability of the free carrier absorption and its relationship to the thermal stabilities of the O-H lines have been examined. Two H-related donors are found, one that is stable at room temperature on a time scale of weeks and a second that is stable up to 600ºC. These electrically active defects are found to interact with other O-H centers and can be converted from one to another by thermal treatments. The vibrational modes have been found to have distinctive polarization properties that provide an important test of microscopic defect models for the several O-H and (O-H)$_2$ centers that we have observed.

# I. INTRODUCTION

The passivation of dopants and defects in semiconductors by hydrogen is well known and has an impact on semiconductor technology that is widely recognized.[1]  Recent theory[2-6] has reinvigorated interest in hydrogen as a possible *source* of conductivity and has drawn attention to early experimental work on H in semiconductors.  For example, in the 1950's hydrogen was known to give rise to shallow donors in ZnO.[7-9]

Transparent conducting oxides have unusual but highly useful properties, combining transparency in the visible region of the spectrum with high electrical conductivity.[10-12]  Native defects such as O vacancies and cation interstitials have been frequently invoked as possible sources of n-type conductivity.[11-14]  Similar to the situation in ZnO, hydrogen recently has been proposed to be an important n-type dopant in several transparent conducting oxides.[4-6,15-18]

$SnO_2$ is a prototypical transparent conducting oxide.[11,12,19]  Recent theory finds that native defects are unlikely to be the source of conductivity.[5]  Instead, interstitial hydrogen[4,5] ($H_i$) and hydrogen at an oxygen vacancy[5] ($H_O$) have been predicted to be donors in $SnO_2$.  $H_i$ has been predicted to be mobile near room temperature whereas $H_O$ has been predicted to be more thermally stable.[5]  The understanding and control of unintentional donor centers in $SnO_2$ is of particular interest because theory also suggests that $SnO_2$ is a good candidate for p-type doping.[5,20]

Early experimental work showed that annealing $SnO_2$ in a hydrogen-containing ambient gives rise to strong n-type conductivity,[21] and a number of O-H absorption lines have been identified in $SnO_2$ minerals.[22-26]  A recent study confirms that annealing $SnO_2$ single crystals in hydrogen increases their conductivity and also gives rise to several O-H vibrational lines with a complicated reaction chemistry upon annealing.[27]  These lines have been assigned to $H_i$ and two different complexes of H with a Sn

2

vacancy.  It was also found that H can be present in $SnO_2$ samples that is not seen by infrared (IR) spectroscopy.  It was suggested that this "hidden" H is present in the form of $H_O$ centers whose vibrational absorption would occur in a spectral region where the sample is opaque.[27]

Our experimental results for H in $SnO_2$ and their interpretation will be compared and contrasted with the properties of H in ZnO.[28]  Both $H_i$ and $H_O$ give rise to shallow donors in ZnO.[2,3,29]  $H_i$ has an O-H vibrational line at 3611 cm$^{-1}$ (ref. 30) and is not thermally stable near room temperature.[31]  When $H_i$ decays upon annealing, $H_2$ molecules are formed that provide a reservoir of hydrogen in the ZnO sample that can be partially converted back to $H_i$ by thermal treatments.[31-33]  $H_O$ is a more thermally stable defect than $H_i$ and decays upon annealing at $\approx 500$ °C.  The $H_O$ donor is believed to be the cause of H-related conductivity in as-grown ZnO materials.[3,29]  Both $H_i$ and $H_O$ can be introduced by annealing a ZnO sample in an $H_2$ ambient at elevated temperatures.  $H_i$ diffuses rapidly and is formed throughout the bulk of a sample that is millimeters thick; $H_O$ has been found to be formed in the near surface region of the sample where O vacancies are also introduced by the annealing treatment.[29]

The present paper reports an IR absorption study of the various hydrogen centers in $SnO_2$, how they are produced, their annealing behavior, and their relationship to the free carriers that are introduced by hydrogen.

II. EXPERIMENT

The $SnO_2$ samples used in our studies were bulk, rutile phase, single crystals that had been grown by the vapor transport method.[34]  To introduce additional hydrogen or deuterium, $SnO_2$ samples were placed in sealed quartz ampoules filled with $H_2$ or $D_2$ gas (2/3 atm at room temperature), annealed at elevated

temperature, and quenched to room temperature in water to terminate the anneals. These anneals in $H_2$ or $D_2$ produced an opaque layer of Sn at the sample surface that was removed by lapping and polishing.

IR absorption spectra were measured with a Bomem DA.3 Fourier transform infrared spectrometer. Light was polarized with a wire grid polarizer that was placed after the sample. O-H and O-D vibrational modes were measured for $SnO_2$ samples at 4.2 K with an InSb detector. Samples were cooled with a Helitran, continuous-flow cryostat. The absorption due to free carriers was measured in our $SnO_2$ samples to provide a contact-free method to probe the free-carrier concentration that is convenient for annealing experiments.

To probe the reactions and thermal stabilities of the various hydrogen-containing centers, annealing treatments were performed in a tube furnace with a flowing He ambient. The O-H lines and free-carrier absorption are not thermally stable for long storage times at room temperature. Therefore, samples were stored at 77 K between measurements except for those experiments where the stabilities of the various hydrogen centers at room temperature were deliberately investigated.

## III. EXPERIMENTAL RESULTS

### A. IR spectra

Figure 1 shows IR spectra (4.2 K) of $SnO_2$ samples that contain H, D, or both H and D. Polarized light with the electric vector perpendicular to the **c** direction was used for these measurements. Spectrum (i) was measured for an as-grown sample and shows a strong O-H line at 3261.5 $cm^{-1}$. Weaker lines are present at 3258.1 and 3272.0 $cm^{-1}$. Spectrum (ii) was measured for a $SnO_2$ sample that was annealed in a He ambient for 30 min at 500°C and quenched rapidly in $D_2O$. ($D_2O$ was used to ensure that the

4

quenching liquid was not the source of H.)  The sample remained optically transparent after this treatment and showed an additional O-H line at 3156.0 cm$^{-1}$.  Similar annealing treatments at 300°C and 700°C also produced the 3156.1 cm$^{-1}$ line but with reduced intensity.  Both spectra (i) and (ii) have flat baselines without any correction.  The annealing treatment at 700°C in a He ambient also produced an IR spectrum with a flat baseline.

Spectrum (iv) was measured for a $SnO_2$ sample that was annealed at 700°C for 30 min in a sealed ampoule containing $H_2$ gas (2/3 atm at room temperature).  The heat treatment was terminated by quenching the ampoule in water.  This anneal in $H_2$ gas caused the sample to partially decompose and damaged the sample surface, producing an opaque layer of Sn on the surface with a thickness of approximately 0.05 mm that was removed by lapping and polishing.  The 3156.1 cm$^{-1}$ line is introduced by this treatment with greater intensity than for spectrum (ii) along with additional lines at 3281.8, 3299.9, 3334.2, and 3343.2 cm$^{-1}$.  This treatment in $H_2$ that severely damaged the $SnO_2$ sample surface also produced the broad low-frequency absorption that arises from the introduction of free carriers,[35] similar to what was found previously for H in ZnO.[32,36,37]

Spectrum (v) was measured for a $SnO_2$ sample that was annealed in a sealed ampoule containing $D_2$ gas (2/3 atm at room temperature) at 700°C for 30 min.  This treatment also damaged the sample surface and produced several O-D lines that are the frequency-shifted partners of the O-H lines seen in spectrum (iv).  The dependence of the line intensities on polarization and annealing treatment (to be shown below) permitted the corresponding O-H and O-D lines to be identified.  Line frequencies are listed in Table I. The ratios of H to D mode frequencies are also shown in Table I and have values close to 1.34, consistent with their assignment to O-H and O-D stretching.  Surprisingly, the treatment in $D_2$ gas also produced the complicated O-H line spectrum that was observed under $H_2$ annealing in spectrum (iv).  The broad absorption due to free carriers is also seen in spectrum (v).

5

Samples used for spectra (i), (ii), (iv), and (v) were in their as-grown state prior to the heat treatment in the ambient that is indicated in Fig. 1. Spectrum (iii), however, was measured for a sample that had been pre-annealed at 1100 °C for 5 hrs in flowing He to remove hydrogen from the as-grown sample. This sample was then annealed in a sealed ampoule containing $D_2$ (2/3 atm at room temperature) at 700 °C for 30 min. Unlike for spectrum (v), in this case, only O-D lines were produced along with the absorption arising from free-carriers.

To investigate whether the O-H and O-D lines and free carriers were from the damaged sample surfaces or from the sample bulk, the sample treated in $D_2$ gas [spectrum (v) in Fig. 1] was mechanically thinned in several steps from a starting thickness of 0.5 mm to a final thickness of 0.2 mm. After each thinning step, an IR spectrum was measured. The O-H and O-D IR lines along with the free carrier absorption were reduced uniformly as the sample was thinned so as to keep the absorption coefficient approximately constant. These results show that the O-H and O-D defects and the free carrier absorption come from defects distributed throughout the sample's initial 0.5 mm thickness.

B. Polarization properties

Figure 2 shows spectra measured with polarized light . This sample had been annealed in $H_2$ gas at 700 °C to produce O-H centers and was subsequently annealed at 100 °C in a He ambient, a treatment that was found to increase the relative intensities of the 3281.8, 3334.2, and 3343.2 cm$^{-1}$ lines in the spectra that are shown. Of the prominent O-H IR lines in the spectrum, the 3156.1 and 3261.5 cm$^{-1}$ lines are polarized perpendicular to the **c**-direction, showing that the O-H bonds for these defects lie in the a-b plane of the rutile structure. The prominent O-H line at 3281.8 cm$^{-1}$ shows absorption for light polarizations both perpendicular and parallel to **c**. (Surprisingly, the intensity of the O-H line at 3281.8 cm$^{-1}$ and its dependence on polarization have been found to depend on the prior annealing treatment of the sample.)

Spectra are shown in Fig. 3 that were measured for an $SnO_2$ sample that had been annealed in a $D_2$ ambient (700 ºC, 30 min) to produce both H- and D-containing centers. We focus first on the O-D frequency region near 2400 cm$^{-1}$. Lines are seen with $\mathbf{E}\perp\mathbf{c}$ at 2360.4, 2425.7, 2432.6, and 2451.3 cm$^{-1}$ (Table I). A line at 2446.9 cm$^{-1}$ is seen for both polarizations, $\mathbf{E}\perp\mathbf{c}$ and $\mathbf{E}//\mathbf{c}$, with an intensity ratio of $I_{//}/I_{\perp} = 0.5$. Upon annealing at 150 ºC, an additional line at 2438.5 cm$^{-1}$ that grows in intensity is seen for polarization $\mathbf{E}\perp\mathbf{c}$.

A comparison of these O-D spectra with the spectra for O-H shown in Fig. 3(b) helps to unravel the unusual behavior of the 3281.8 cm$^{-1}$ line that occurs upon annealing. In the as-treated sample, the ratio, $I_{//}/I_{\perp}$ for the 3281.8 cm$^{-1}$ line is similar to that of the corresponding O-D line at 2446.9 cm$^{-1}$ seen in Fig. 3(a). Upon annealing at 150 ºC, the intensity of the 3281.8 cm$^{-1}$ line grows primarily for $\mathbf{E}\perp\mathbf{c}$. A comparison of the results shown in Figs. 3(a) and 3(b) and their annealing behavior shows that the lines at 2438.5 and 2446.4 cm$^{-1}$, that are separate in the O-D spectrum, have isotopic partners in the O-H spectrum that lie at the same frequency, 3281.8 cm$^{-1}$. The coincidence of two O-H modes with different polarization properties and annealing behaviors explains the unusual changes in the ratio $I_{//}/I_{\perp}$ for the 3281.8 cm$^{-1}$ line upon annealing.

There are additional prominent O-H absorption lines seen in our experiments. When a hydrogenated sample is annealed near 100 to 150 °C (Figs. 2 and 3), the IR lines at 3334.2 and 3343.2 cm$^{-1}$, that were initially present only weakly, grow in intensity. These lines have distinct polarization properties (Fig. 2), with the 3334.2 cm$^{-1}$ line seen only for $\mathbf{E}//\mathbf{c}$ and the 3343.2 cm$^{-1}$ line seen only for $\mathbf{E}\perp\mathbf{c}$. The corresponding O-D lines seen for a sample treated in a $D_2$ ambient have the same polarization behavior and lie at 2477.5 and 2483.8 cm$^{-1}$ (Table I).

Results from the previous study by Hlaing Oo et al.[27] differ from the above, and O-H absorption was reported only for **E⊥c.** Furthermore, the lines at 3334.2 and 3343.2, while present, were weak in the spectra reported by Hlaing Oo et al. and were not discussed in their paper.[27]


C. Annealing behavior


A series of annealing experiments has been performed to investigate the thermal stabilities of the free-carrier absorption and also the various O-H and O-D centers. Figure 4(a) shows free-carrier absorption spectra that were measured at room temperature for a sample treated in $H_2$ gas following a series of subsequent heat treatments in a He ambient at the temperatures shown. Each anneal was terminated by a rapid quench to room temperature. The difference between the absorbances at 2000 cm$^{-1}$ and 4000 cm$^{-1}$ is taken to be a measure of the strength of the free-carrier absorption and is plotted as a function of the annealing temperature in Fig. 4(b). The annealing of the free carrier absorption shows an interesting dependence on the heat-treatment temperature. Annealing the sample for 30 min at temperatures between 100 and 150 °C causes the free-carrier absorption to be reduced by nearly 25%. Anneals at temperatures $\geq$ 200 °C caused the free carrier absorption seen prior to annealing near 100 °C to be recovered. Upon further annealing at higher temperatures, the majority of the free-carrier absorption was finally eliminated by an anneal at 650 °C.


Figure 5 shows a selection of IR spectra (4.2 K) for the O-H centers that were present for the same sequence of anneals whose free-carrier data are shown in Fig. 4. (These O-H spectra were baseline corrected to remove the absorption due to free carriers.) The areas of the individual absorption lines were determined by fitting the spectra with sums of Lorentzian line shapes. A plot of the areas of the dominant lines vs. the annealing temperature is shown in Figs. 6(a) and 6(b). The temperature dependence of the free-carrier absorption is shown in Fig. 6(c) for comparison.

Figure 7(a) shows the stability of the free-carrier absorption after a sample that had been treated in an H$_2$ ambient (700 ºC, 30 min) was "annealed" for long times at room temperature. The strength of the free-carrier absorption was reduced by nearly 35% after 65 days at room temperature and was not reduced further after 108 days. Figure 7(b) shows the corresponding, baseline-corrected, O-H spectra. In this case, the intensity of the 3156.1 cm$^{-1}$ line was nearly eliminated following storage for times of 65 days and longer. Over the same time period, the intensity of the 3261.5 cm$^{-1}$ line was reduced by 24% while the intensities of the 3281.9 and 3343.2 cm$^{-1}$ lines were increased.

After the sample had been stored for 108 days at room temperature, it was re-annealed at 500 °C for 30 min in flowing He followed by a rapid quench. Following this heat treatment, the initial free-carrier absorption was recovered and the intensities of the 3156.5 and 3261.5 cm$^{-1}$ lines were increased at the expense of the other O-H absorption lines in the sample. Furthermore, the total intensity of all of the O-H lines was found to be nearly constant for the various spectra shown in Figure 7, that is, for the as-treated sample, following the subsequent storage times at room temperature, and following heat treatment at 500 °C. This result suggests that the various O-H centers have IR lines with similar oscillator strengths and that these centers can be inter-converted into one another by the appropriate thermal treatments.

IV. DISCUSSION

A. Production and thermal stability of H-related shallow donors

Samson and Fonstad found that annealing SnO$_2$ in an H$_2$ containing ambient at 900 °C introduced shallow donors with concentrations between 9.8x10$^{17}$ and 8x10$^{18}$ cm$^{-3}$, depending on the sample, and suggested that H was the shallow donor.[21] The spectra shown in the present work in Figs. 1 and 4 show that annealing SnO$_2$ in an H$_2$ ambient at 700 °C produces strong free-carrier absorption in addition to a

number of O-H vibrational lines, in agreement with other recent work.[27] SnO$_2$ and ZnO have similar electron masses and mobilities[19, 38, 39] suggesting that calibrations of the free-carrier absorption determined previously for ZnO,[32, 36, 37] also annealed in an H$_2$ ambient, can be applied approximately to the free-carrier absorption spectra measured for SnO$_2$ at room temperature.[40] With this approximate calibration, the free-carrier absorption shown in the "as-treated" spectrum in Fig. 4 corresponds to an electron concentration of $\approx 1 \times 10^{18}$ cm$^{-3}$, similar to the early results of Samson and Fonstad.[21]

The strong free-carrier absorption and large concentration of shallow donors ($\approx 10^{18}$ cm$^{-3}$) were only produced in SnO$_2$ samples that were annealed in an H$_2$ or D$_2$ ambient. If donors were produced in SnO$_2$ samples annealed at 700°C in a He ambient, our free-carrier absorption studies show that their concentration was at least 5 to 10 times smaller than the donor concentration produced by annealing in H$_2$.

The annealing stabilities of the H-related donors in SnO$_2$ (Figs. 4 and 7) suggest that there are at least two H-related donors. The dip in the free-carrier absorption at 100 °C seen in the annealing data shown in Fig. 4(b) suggests that there is a donor species that is not thermally stable at this temperature. There is also an additional shallow donor that is stable up to an annealing temperature of 650 °C where the majority of the free carrier absorption due to H disappears. The spectra shown in Fig. 7(a) further support the conclusion that two donor species are present with different thermal stabilities. When a hydrogenated sample is held for 65 days at room temperature, the free-carrier absorption, measured in this case at 4.2 K, is reduced by 35%. This fraction accounts for the donor that is not stable at room temperature. The free-carrier absorption that remains is more thermally stable and does not decay appreciably for longer times at room temperature.

B. Relationship of shallow donors to hydrogen centers


The annealing data shown in Figs. 5, 6, and 7 help to identify the various hydrogen centers.  The

annealing results in Figs. 5 and 6 show that the dip in the free-carrier absorption that occurs for annealing

at 100 to 150 °C is correlated with a corresponding reduction in the intensity of the O-H line at 3156.1

cm$^{-1}$.  The spectra in Fig. 7 lead to the same conclusion.  The intensity of the IR line at 3156.1 cm$^{-1}$shows

a reduction in intensity similar to that of the component of the free-carrier absorption that is not stable for

a long storage time at room temperature.  When this sample was annealed at 500 °C in a He ambient and

quenched, the free-carrier absorption and the 3156.1 cm$^{-1}$ line recovered together.


Theory has shown that the $H_i$ center is a shallow donor[4, 5] and that this defect is mobile near room

temperature.[5,27]  A strong O-H bond is predicted that lies perpendicular to the **c**-axis with a theoretical

vibrational frequency of 3245 cm$^{-1}$.[20,27]  The correspondence of these predicted properties to the

experimental behavior of the O-H center that gives rise to the 3156.1 cm$^{-1}$ line led Hlaing Oo *et al.* to

assign the 3156.1 cm$^{-1}$ line to $H_i$.[27]  Our results for the 3156.1 cm$^{-1}$ line's vibrational properties, its

thermal stability, and the close correspondence of this line to the free-carrier absorption in annealing

experiments strongly support this assignment.


Theory predicts that $H_O$ is also a donor in $SnO_2$ but with greater thermal stability than $H_i$.[5,27]  $H_O$ is,

therefore, an excellent candidate for the cause of that portion of the free carrier absorption that we have

found to be stable up to near 650 °C for samples that had been heat treated in an $H_2$ ambient to introduce

H.


Our results for H in $SnO_2$ are similar to what has been found previously for H in ZnO where $H_i$, with

an O-H vibrational line at 3611 cm$^{-1}$, and $H_O$ both act as shallow donors.[29]  In ZnO that had been annealed

in an $H_2$ ambient at 700 °C, approximately 85% of the donors that were formed were not thermally stable

near room temperature and only 15% were stable up to near 500 °C.[31]  In ZnO, $H_O$ was found to be

formed in the near surface region of a sample treated in $H_2$ at temperatures near 700 °C.[29]


For $SnO_2$, we have introduced hydrogen with annealing treatments in $H_2$ that severely damage the

sample surface.  In these experiments, $H_i$ and $H_O$ are introduced deep into the bulk of the $SnO_2$ sample,

and $H_O$ is the dominant donor (≈65%) following hydrogenation.  This result shows that the oxygen

vacancies necessary for the production of the $H_O$ donor center are introduced deep into the sample bulk by

the damaging anneal in an $H_2$ ambient.


C. Properties of other O-H centers


The O-H stretching spectrum contains a number of IR lines in addition to the line at 3156.1 $cm^{-1}$.  The

similarity of the spectra reported in the present paper to those reported recently by Hlaing Oo *et al.*[27] for a

different source of samples suggests that most of these lines are due to O-H centers that involve H and

intrinsic defects rather than additional impurities that might be expected to depend on the sample source.

(The few weaker lines that do differ, for example a line at 3294 $cm^{-1}$ seen by  Hlaing Oo *et al.*[27] but not by

us, may indeed be due to H trapped in the vicinity of other impurities.)


Polarized spectra for a sample containing both H and D provide additional clues to the identity of the

O-H and O-D centers.  Fig. 3(b) shows that an additional line appears at 3339.0 $cm^1$, midway between the

3334.2 and 3343.2 $cm^{-1}$ lines, for both $E \perp c$ and $E // c$ for a sample that contains both H and D.  This

behavior is characteristic of a center that contains two equivalent H atoms.  The line that appears at

3339.0 $cm^{-1}$ is assigned to the dynamically decoupled O-H mode that is present when one of the H atoms

of this $(O-H)_2$ center has been replaced by D.  Similarly, the lines seen in the O-D stretching spectrum at

2477.5 and 2483.8 $cm^{-1}$ [Fig. 3(a)] are due to this same defect except with two D atoms substituted for H.

The dynamically decoupled O-D mode for this center when it contains both H and D lies at 2479.7 $cm^{-1}$.

12

The formation of an $(O\text{-}H)_2$ complex in $SnO_2$ is still another similarity to the behavior of H in ZnO where a complex of two H atoms with a zinc vacancy $(V_{Zn}\text{-}H_2)$ has been identified.[30, 41]  In the present paper, we are concerned primarily with $(O\text{-}H)_2$ as a source and sink for H in annealing experiments. Candidates for possible microscopic defect structures will be discussed elsewhere.

The other O-H lines in the spectra for a sample containing both H and D do not give rise to additional, dynamically decoupled components when D is partially substituted for H.  All of the O-H lines we have seen, other than the 3334.2 and 3343.2 cm$^{-1}$ lines discussed above, show behaviors characteristic of defects that contain a single H atom.  The mode assignments and their polarization properties are summarized in Table I.

The polarization properties of the IR lines provide important clues to the mode assignments.  For example, candidates for the O-H lines at 3261.7 and 3281.8 cm$^{-1}$ that have been suggested by theory[27] are complexes of hydrogen with a $V_{Sn}$.  There are two possible configurations for the $V_{Sn}$-H complex, the first with H bonded to one of the Sn vacancy's axial O neighbors to form an O-H bond that is perpendicular to **c** and the second with H bonded to one of the Sn vacancy's equatorial O neighbors.[27]  The polarizations of the IR lines would be consistent with the 3261.7 cm$^{-1}$ line that is seen for $\mathbf{E}\perp\mathbf{c}$ being assigned to H bonded to one of the $V_{Sn}$ defect's axial O neighbors.  The 3281.8 cm$^{-1}$ line that is seen for both $\mathbf{E}\perp\mathbf{c}$ and $\mathbf{E}//\mathbf{c}$ would be qualitatively consistent with an assignment to H bonded to one of the $V_{Sn}$ defects equatorial O neighbors.  (These assignments, based on the polarization properties of the IR lines, are reversed from the defect assignments suggested by Hlaing Oo *et al.*[27])

Other possible assignments of these O-H modes will be discussed elsewhere.

D. Sources and sinks for hydrogen.

Our data show that there are hydrogen centers in our as-grown $SnO_2$ samples that do not give rise to electrically active shallow donors. Simply annealing an as-grown sample in a He ambient and quenching produces a small concentration of $H_i$ [spectrum (ii) in Fig. 1]. When a sample is annealed in an $H_2$ ambient, $H_i$, $H_O$, and additional O-H defects are produced throughout the sample bulk [spectrum (iv) in Fig. 1]. What is surprising is that when an as-grown sample is annealed in a $D_2$ ambient [spectrum (v) in Fig. 1], not only are deuterium centers formed, but *hydrogen* centers are again formed throughout the bulk of the $SnO_2$ sample from the interaction of hydrogen that was already present with native defects that are introduced by the heat treatment. After an $SnO_2$ sample is annealed at elevated temperature (1100 °C) to remove H, annealing in a $D_2$ ambient produces deuterium centers but does not produce hydrogen centers [spectrum (iii) in Fig. 1], supporting the conclusion that O-H centers can be produced from H already present in an as-grown sample. These results, in which H already present in the sample can be converted into shallow donors and O-H centers by a heat treatment in a $D_2$ ambient, demonstrate the dual role played by the damaging anneal in $D_2$ as both a source of native defects that form the defect centers seen in our experiments and as a source of deuterium.

Hlaing Oo *et al.* have suggested that $H_O$ is a possible source of hidden hydrogen in $SnO_2$ samples.[27] However, because of the electrical activity of the $H_O$ center, it cannot explain the reservoir of H that is present in our samples that does not give rise to strong free-carrier absorption. One possible source of H in as-grown samples is the O-H center with its IR line at 3261.5 cm$^{-1}$. (Other O-H centers are not prominent in as-grown samples.) Another possibility for a source of hydrogen in as-grown $SnO_2$ samples is the $H_2$ molecule. Theory predicts that $H_2$ has a high formation energy in $SnO_2$.[27] Our experimental data that reveal an electrically inactive source of H, however, suggest that $H_2$ remains an attractive candidate for a source of hidden hydrogen in our experiments that does not give rise to free-carrier absorption or O-H vibrational lines, similar to the role played by $H_2$ in ZnO.[32,33]

Once a sample has been heat treated at elevated temperature in a $H_2$ or $D_2$ ambient, the H- or D-containing centers that are formed are found to exchange H or D with one another. The data in Figs. 4, 5 and 7 show that there are hydrogen centers that give rise to electrically active shallow donors that can be converted into centers that do not and vice versa. The data in Fig. 7, for example, show that during long storage times at room temperature, the IR lines at 3261.5, 3281.8, 3334.2 and 3343.2 $cm^{-1}$ that are assigned to O-H and $(O-H)_2$ complexes change in intensity as the free-carrier absorption and the IR line at 3156.1 $cm^{-1}$ associated with the $H_i$ shallow donor disappear. When this sample was subsequently annealed at 500 °C in a He ambient and quenched, $H_i$ recovered at the expense of the H trapped in other $(O-H)_n$ complexes and the 3261.5 $cm^{-1}$ line also regained its intensity. These results show that the $H_i$ and $(O-H)_n$ centers can be converted into one another. The changes in the line intensities suggest that $H_i$ migrates to be trapped by a native defect to form the 3281.8 $cm^{-1}$ center. The decrease of the 3261.5 $cm^{-1}$ line with the concomitant increase of the 3334.2 and 3343.2 $cm^{-1}$ lines assigned to $(O-H)_2$ suggests that the O-H center that gives rise to the 3261.5 $cm^{-1}$ line traps an additional H atom to form an $(O-H)_2$ center. Annealing at elevated temperature (500 ºC here) releases $H_i$ from these defects that becomes trapped as the isolated interstitial donor species when the sample is quickly quenched to room temperature.

Hydrogen from the more stable shallow donor that has been proposed to be due to $H_O$ can also be converted into other defects upon annealing. The data in Fig. 6 show that as the free-carrier absorption that arises from the $H_O$ center is annealed away at 600 °C, the $H_i$ center (3156.1 $cm^{-1}$ line) and the O-H center that gives rise to the 3261.5 $cm^{-1}$ line grow in intensity.

V. CONCLUSION

The properties of H in single crystals of the transparent conducting oxide $SnO_2$ have been studied with IR spectroscopy. When H is introduced into $SnO_2$ by annealing in an $H_2$ ambient at elevated

15

temperature, O-H vibrational lines are produced along with the low-frequency absorption that is characteristic of free carriers. An anneal in an $H_2$ ambient has been found to play a dual role, introducing both the hydrogen and the native defects that form shallow donors and O-H centers throughout the bulk of the $SnO_2$ sample. Furthermore, when an as-grown $SnO_2$ sample is annealed in a $D_2$ ambient, O-H centers and shallow donors are formed from electrically inactive hydrogen that was already present in the sample.

To probe the relationship between H and the free carriers it introduces, the thermal stability of the free carrier absorption and its relationship to the thermal stabilities of the various O-H centers have been studied. Two H-related donors are found, one that is only marginally stable at room temperature and a second that is stable up to 600ºC. A vibrational line at 3156.1 cm$^{-1}$ that was assigned previously by Hlaing Oo *et al.*[27] to interstitial H has an annealing behavior that is consistent with its being the less stable donor species. The more stable donor is not seen by vibrational spectroscopy and has a thermal stability that is consistent with its being the $H_O$ center (H trapped at an oxygen vacancy) that was predicted by theory.[5,27]

The vibrational properties and chemical reactions of several O-H centers have been studied. An (O-H)$_2$ center has been discovered in IR experiments performed for $SnO_2$ samples that contained both H and D. The electrically active hydrogen donors are found to interact with these O-H and (O-H)$_2$ centers and can be inter-converted from one into another by thermal treatments. These results show that when $SnO_2$ contains hydrogen, its conductivity will be highly sensitive to the thermal history of the sample.

The vibrational modes of the several O-H and (O-H)$_2$ centers that have been observed in $SnO_2$ have been found to have distinctive polarization properties that provide an important, structure-sensitive test of any microscopic defect models that might be proposed.

## VI. Acknowledgment

## References

*mjsa@Lehigh.edu

1. S. J. Pearton, J. W. Corbett, and M. Stavola, *Hydrogen in Crystalline Semiconductors*, (Springer-Verlag, Heidelberg, 1992).

2. C. G. Van de Walle, Phys. Rev. Lett. **85**, 1012 (2000).

3. A. Janotti and C. G. Van de Walle, Nature Materials **6**, 44 (2007).

4. C. Kiliç and A. Zunger, Appl. Phys. Lett. **81**, 73 (2002).

5. A. K. Singh, A. Janotti, M. Scheffler, C. G. Van de Walle, Phys. Rev. Lett. **101**, 055502 (2008).

6. S. Limpijumnong, P. Reunchan, A. Janotti, and C. G. Van de Walle, Phys. Rev. B **80**, 193202 (2009).

7. E. Mollwo, Z. Phys. **138**, 478 (1954); G. Heiland, E. Mollwo, and F. Stöckman, in *Solid State Physics*, edited by F. Seitz and D. Turnbull (Academic Press, New York, 1959) Vol. 8, p. 193.

8. D. G. Thomas and J. J. Lander, J. Chem. Phys. **25**, 1136 (1956).

9. A. R. Hutson, Phys. Rev. **108**, 222 (1957).

10. G. Thomas, Nature **389**, 907 (1997).

11. H. L. Hartnagel, A. L. Dawar, A. K. Jain, C. Jagadish, *Semiconducting Transparent Thin Films* (Institute of Physics, London, 1995).

12. *Transparent Electronics: From Synthesis to Applications*, edited by A. Facchetti and T. Marks (Wiley, New York, 2010).

13. C. Kiliç and A. Zunger, Phys. Rev. Lett. **88**, 095501 (2002).

14. P. Ágoston, K. Albe, R. Nieminen, and M. Puska, Phys. Rev. Lett. **103**, 245501 (2009).

15. S. F. J. Cox**,** J. S. Lord, S. P. Cottrell, J. M. Gill, H. V. Alberto, A. Keren, D. Prabhakaran, R. Scheuermann, and A. Stoykov, J. Phys.: Condens. Matter **18**, 1061 (2006).

16. S. F. J. Cox, J. L. Gavartin, J. S. Lord, S. P. Cottrell, J. M. Gill, H. V. Alberto, J. Piroto Duarte, R. C. Vilão, N. Ayres de Campos, D. J. Keeble, E. A. Davis, M. Charlton, and D. P. van der Werf, J. Phys.: Condens. Matter **18**, 1079 (2006).

17. P. D. C. King, R. L. Lichti, Y. G. Celebi, J. M. Gil, R. C. Vilão, H. V. Alberto, J. Piroto Duarte, D. J. Payne, R. G. Egdell, I. McKenzie, C. F. McConville, S. F. J. Cox, and T. D. Veal, Phys. Rev. B **80**, 081201 (R) (2009).

18. P. D. C. King, I. McKenzie, and T. D. Veal, Appl. Phys. Lett. **96**, 062110 (2010).

19. Z. M. Jarzebski and J. P. Marton, J. Electrochem. Soc. **123**, 299C (1976).

20. J. B. Varley, A. Janotti, A. K. Singh, and C. G. Van de Walle, Phys. Rev. B **79**, 245206 (2009).

21. S. Samson and C. G. Fonstad, J. Appl. Phys. **44**, 4618 (1973).

22. R. S. Katiyar, P. Dawson, M. M. Hargreave, G. R. Wilkinson, J. Phys. C: Solid St. Phys. **4**, 2421 (1971).

23. A. Beran and J. Zemann, Tschermaks Min. Petr. Mitt. **15**, 71 (1971).

24. F. Bréhat, B. Wyncke, J.M. Léonard and Y. Dusausoy, Phys. Chem. Minerals **17**, 191 (1990).

25. J. Maldener, F. Rauch, M. Gavranic, and A. Beran, Mineral. Petrol. **71**, 21 (2001).

26. Z. Losos and A. Beran, Mineral. Petrol. **81**, 219 (2004).

27. W. M. Hlaing Oo, S. Tabatabaei, M. D. McCluskey, J. B. Varley, A. Janotti, and C. G. Van de Walle, Phys. Rev. B **82**, 193201 (2010).

28. M. D. McCluskey and S. J. Jokela, J. Appl. Phys. **106**, 106 (2009).

29. E. V. Lavrov, F. Herklotz, and J. Weber, Phys. Rev. B **79**, 165210 (2009).

30. E. V. Lavrov, J. Weber, F. Börnnert, C. G. Van de Walle, and R. Helbig, Phys. Rev. B **66**, 165205 (2002).

31. G. A. Shi, M. Stavola, S. J. Pearton, M. Thieme, E. V. Lavrov, and J. Weber, Phys. Rev. B **72**,195211 (2005).

32. G. A. Shi, M. Saboktakin, M. Stavola, and S. J. Pearton, Appl. Phys. Lett. **85**, 5601 (2004).

33. E. V. Lavrov, F. Herklotz, and J. Weber, Phys. Rev. Lett. **102**, 185502 (2009).

34. B. Thiel and R. Helbig, J. Crystal Growth **32**, 259 (1976).

35. P. Y. Yu and M. Cardona, *Fundamentals of Semiconductors, Physics and Materials Properties* (Springer, Berlin, 2010), 4th ed.

36. D. G. Thomas, J. Phys. Chem. Solids **10**, 47 (1959).

37. C. H. Seager and S. M. Myers, J. Appl. Phys. **94**, 2888 (2003).

38. S. J. Pearton, D. P. Norton, K. Ip, and Y. W. Heo, J. Vac. Sci. Technol. B **22**, 932 (2004).

39. C. Klingshirn, Phys. Stat. Sol. (b) **244**, 3027 (2007).

40. The calibration of the free carrier absorption coefficient at 2000 cm$^{-1}$ given in reference (32) for hydrogenated ZnO is $n_{fc} = 9.3 \times 10^{15}$ cm$^{-2}$ $\alpha$(2000 cm$^{-1}$).

41. D. Bastin, E. V. Lavrov, and J. Weber, Phys. Rev. B, in press.

Table I. Frequencies of O-H and O-D vibrational modes observed for an $SnO_2$ sample that had been annealed in $H_2$ or $D_2$ gas. The ratio r of the O-H and O-D line frequencies and the polarization ratio $I_{//} / I_{\perp}$ for the various lines are also shown.

| $\omega_H$ | $\omega_D$ | r | assignment | $I_{//} / I_{\perp}$ |
|---|---|---|---|---|
| 3156.1 | 2360.4 | 1.337 | $H_i$ | 0 |
| 3258.1 | ----- | ----- | O-H | 0 |
| 3261.5 | 2425.7 | 1.345 | O-H | 0 |
| 3272.0 | 2432.6 | 1.345 | O-H | 0 |
| 3281.8 | 2438.5 | 1.346 | O-H | 0 |
| 3281.8 | 2446.9 | 1.341 | O-H | 0.5 |
| 3299.9 | 2451.3 | 1.346 | O-H | 0 |
| 3334.2 | 2477.5 | 1.346 | $(O-H)_2$ | 1 |
| 3343.2 | 2483.8 | 1.346 | $(O-H)_2$ | 0 |

**Figure captions**

FIG. 1.  IR absorption spectra (T=4.2 K, resolution=1 cm$^{-1}$) for SnO$_2$ samples that had been annealed (30 min) in the ambient and at the temperatures that are indicated.  The sample for spectrum (iii) had been preannealed at 1100 °C for 5 hours to remove H from the sample prior to an anneal in a deuterium ambient.  (a) shows both the absorption due to free carriers and due to O-H and O-D centers.  (An empty sample holder was used as the reference for these data.)  (b) shows the IR lines in the O-H stretching region.  These spectra were baseline corrected to remove the contribution from free-carriers.

FIG. 2.  IR absorption spectra (T=4.2 K, resolution=1 cm$^{-1}$) measured for light polarized with electric vector **E**⊥**c** and with **E**//**c**.  H was introduced by an anneal (30 min) in H$_2$ gas at 700 °C.  The sample was subsequently annealed (30 min) at 100 °C in a He ambient.

FIG. 3.  IR absorption spectra (T=4.2 K, resolution=1 cm$^{-1}$) measured for light polarized with electric vector **E**⊥**c** (upper) and with **E**//**c** (lower).  D was introduced by an anneal (30 min) in D$_2$ gas at 700 °C for the "as-treated" sample.  The sample was subsequently annealed (30 min) at 150 °C in a He ambient. (a) shows the O-D stretching region.  (b) show the O-H stretching region.  The line at 3261.5 (2425.7) was truncated so that weaker lines in the spectrum could be seen more clearly.

FIG. 4.  (a) Selection of free-carrier absorption spectra (room temperature, resolution=1 cm$^{-1}$) measured for a single-crystal SnO$_2$ sample.  The sample was first annealed (30 min) at 700 °C in H$_2$ gas to introduce H.  The sample was subsequently annealed in a He ambient at the temperatures shown.  Anneals were terminated by a quench to room temperature in water.  The reference spectrum for these data (not shown) was measured for the same sample following an anneal at 900 °C in a He ambient that was performed to

21

remove H.  (b) Difference in the absorption coefficients measured at 2000 cm$^{-1}$ and 4000 cm$^{-1}$ vs. the annealing temperature.

FIG. 5.  Baseline corrected IR absorption spectra (T=4.2 K, resolution=1 cm$^{-1}$) for the SnO$_2$ sample whose free-carrier absorption data are shown in Fig. 4.  The sample was first annealed (30 min) at 700 °C in H$_2$ gas to introduce H.  The sample was subsequently annealed in a He ambient at the temperatures shown.  Anneals were terminated by a quench to room temperature in water.  The sample was then sequentially annealed (30 min) in a flowing He ambient at the temperatures shown.  Anneals were terminated by a quench to room temperature in water.  Spectra were measured with polarized light with **E**⊥**c**.

FIG. 6.  Panels (a) and (b) show the integrated absorption coefficients for the IR lines at the frequencies indicated vs annealing temperature.  Anneals (30 min) were performed in a flowing He ambient and were terminated by a rapid quench to room temperature.  Open and closed squares in panel (a) and open and closed circles in panel (b) are for **E**⊥**c**.  Open and closed triangles in panel (b) are for **E**//**c**.  (c) shows the difference in the absorption coefficients due to free carriers measured at 2000 cm$^{-1}$ and 4000 cm$^{-1}$ vs. the annealing temperature.  Line are drawn to guide the eye.

FIG. 7.  IR absorption spectra (T=4.2 K, resolution=1 cm$^{-1}$) for an SnO$_2$ sample that had been annealed (30 min) at 700 °C in H$_2$ gas to introduce H.  The sample was subsequently held at room temperature for the times that are indicated.  (a) shows both the absorption due to free carriers and due to O-H centers.  (b) shows the IR lines in the O-H stretching region.  These spectra were baseline corrected to remove the contribution from free-carriers.
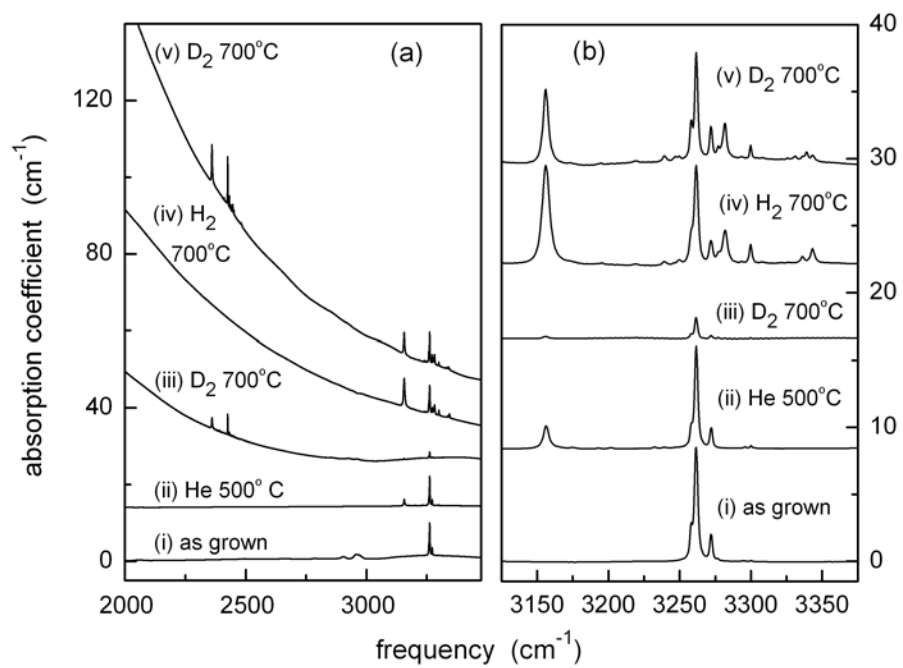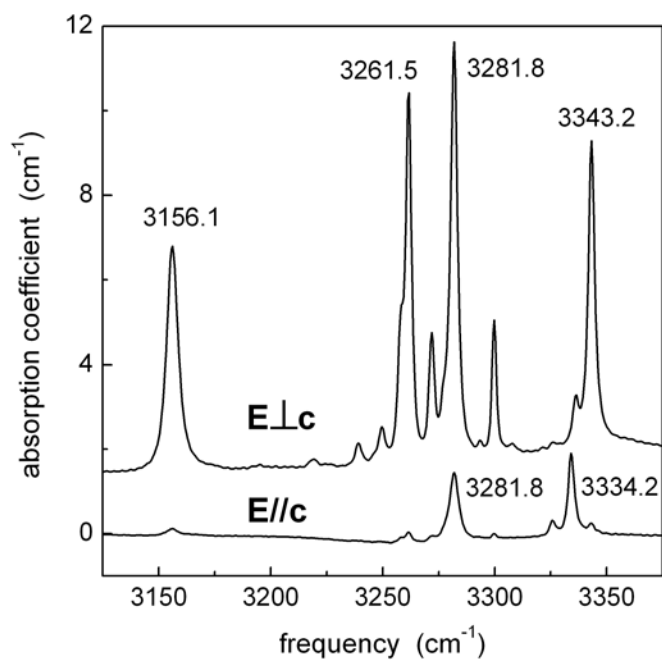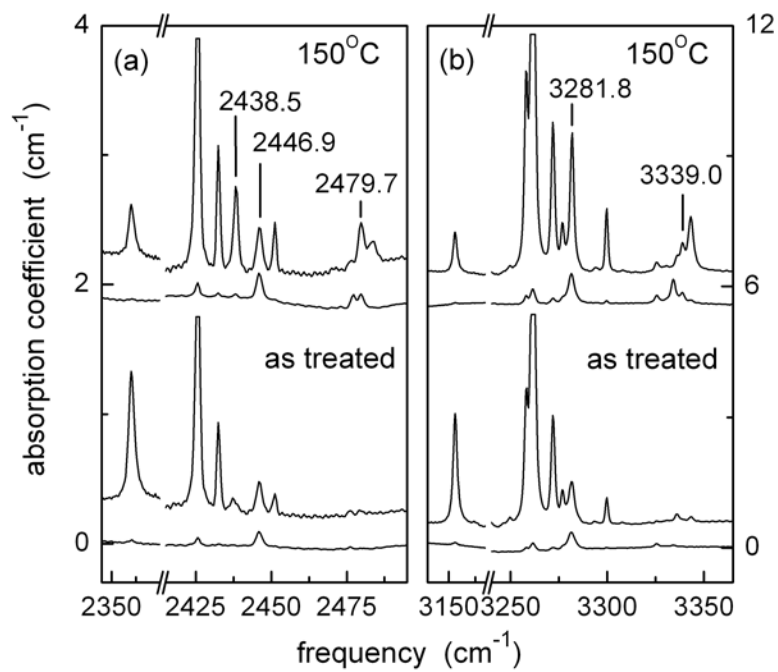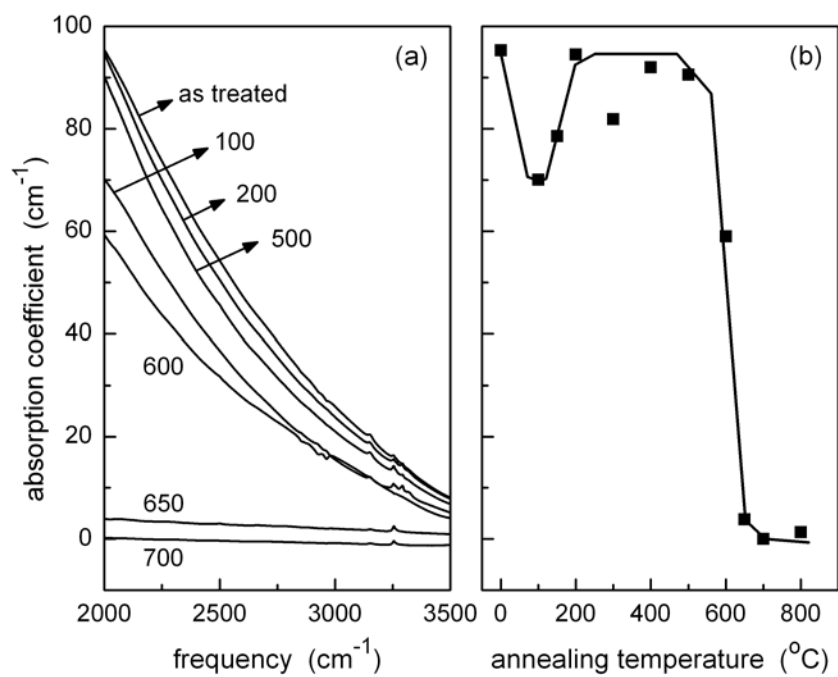
Fig. 1



Fig. 2

Fig. 3



Fig. 4

24

Fig. 5



Fig. 6

Fig. 7